

# Observation of turbulent intermittency scaling with magnetic helicity in an experimental MHD plasma

D.A. Schaffner,<sup>1</sup> A. Wan,<sup>1</sup> and M.R. Brown<sup>1</sup>  
*Swarthmore College, Swarthmore, PA, USA*

(Dated: 21 November 2013)

The intermittency in turbulent magnetic field fluctuations has been observed to scale with the amount of magnetic helicity injected into an experimental flux rope plasma. A selectively decayed Taylor state is created in the wind-tunnel configuration of the Swarthmore Spheromak Experiment using a stuffed plasma gun. The amount of flux in the core of the gun can be varied linearly which in turn modifies the amount of helicity injected into the plasma. The level of intermittency is determined by finding the flatness (4th order moment) of the probability distribution function of increments for magnetic fluctuations. This higher order aspect of the turbulence is observed to increase with the injected helicity while the spectral index in the inertial range of the turbulence appears to be unaffected by this variation. Some experimental evidence is given for the role of current sheets and reconnection sites in the generation of this intermittency, but the true nature of the observed intermittency remains unknown.

The study of magnetic turbulence in laboratory experiment and in space plasmas has been conducted using a multitude of approaches including the construction and analysis of power spectra, correlations and probability distribution functions for both temporal and spatial datasets<sup>27</sup>. Much focus has been placed on studying power spectra, or really, the rate of transfer of energy from large scales to small scales reflected in the spectral index, as this quantity has the most intuitive physical reason and firmest connection to the Kolmogorov theory of fluid turbulence. However, examination of power spectra follows only one thread of insight into the characteristics that make up a turbulent plasma. The role of intermittency in turbulence theory has developed alongside spectral theory in fluid mechanics<sup>25</sup> and has become an integral aspect of turbulence analysis in both space<sup>10–12</sup> and laboratory plasmas<sup>31,32</sup>.

This paper presents the results of an experimental scan which establishes a connection between a controllable experimental quantity—magnetic helicity—and a turbulent characteristic—intermittency—as well as highlights the need for a multi-pronged approach to turbulence analysis. The experimental scan was conducted on the wind-tunnel configuration of the Swarthmore Spheromak Experiment which consists of a 86cm long by 15.5cm wide cylindrical copper flux conserver into which a plasma gun (shown in Figure 1) injects dense, highly magnetized ( $\sim 1 \times 10^{15} \text{cm}^{-3}$ ,  $\sim 5 \text{kG}$ ) plasma which self-organizes into a Taylor state<sup>3</sup>. The injected magnetic helicity of the plasma can be modified by setting the amount of flux through the plasma gun using a coaxial magnetic coil. Power spectra and probability density functions of increments are constructed using fluctuation magnetic data extract from pickup coils ( $\dot{B}$  probes) inserted radially into the flux conserver at the midplane. While power-law fits to the power spectra show no scaling with the change in helicity, the turbulent intermittency, as indicated by the calculated flatness of the PDFs, increases with the helicity with flatness values ranging from near Gaussian ( $F \sim 5$ ) to values over 30.

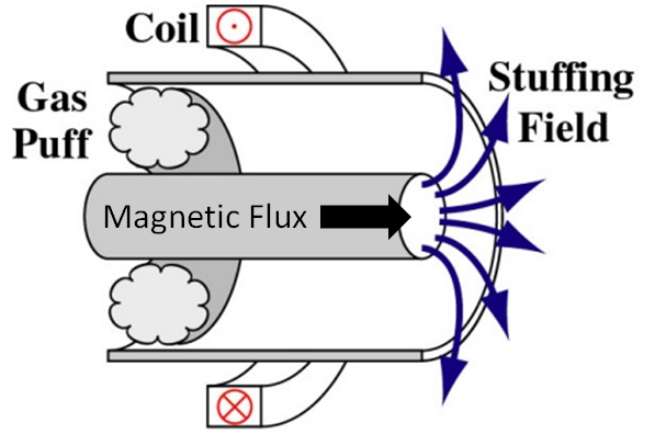


FIG. 1. Diagram of the plasma gun attached to one end of the copper flux conserver in SSX. The diagram shows how the magnetic flux in the core of the gun is modified by adjusting the current in the coil outside of the gun which sets up the stuffing field.

The injection of magnetic helicity into the plasma is a natural consequence of the formation procedure for a plasma gun. Magnetic helicity,

$$K_B = \int A \cdot B dV \quad (1)$$

is a measure of the amount of twistedness of the magnetic field lines and can be expressed in terms of magnetic flux squared (i.e. units of  $Wb^2$ ). This quantity can be recast in a more experimentally relevant quantity,

$$K_B = \int \Phi V_{gun} dt \quad (2)$$

where  $\Phi$  is the magnetic flux penetrating the plasma gun core and  $V_{gun}$  is the voltage drop across the gun gap. This is the form of the helicity that is calculated and reported as in this paper. Since the plasma forms under

the assumption of selective decay (conservation of magnetic helicity) are reported in Gray 2013<sup>[3]</sup>, it is further assumed that the amount of helicity injected by the gun is conserved and present in the plasma under observation. Though the voltage across the gun gap is recorded for the entire duration of the shot, only the first  $20\mu s$  are used to estimate the injected helicity. Beyond  $20\mu s$ , the voltage measurement is significantly affected by breaking fieldlines during spheromak formation. Though it is assumed that helicity injection is nearly constant for the duration of the discharge, the values of helicity reported here is that for the first  $20\mu s$  after the initial trigger.

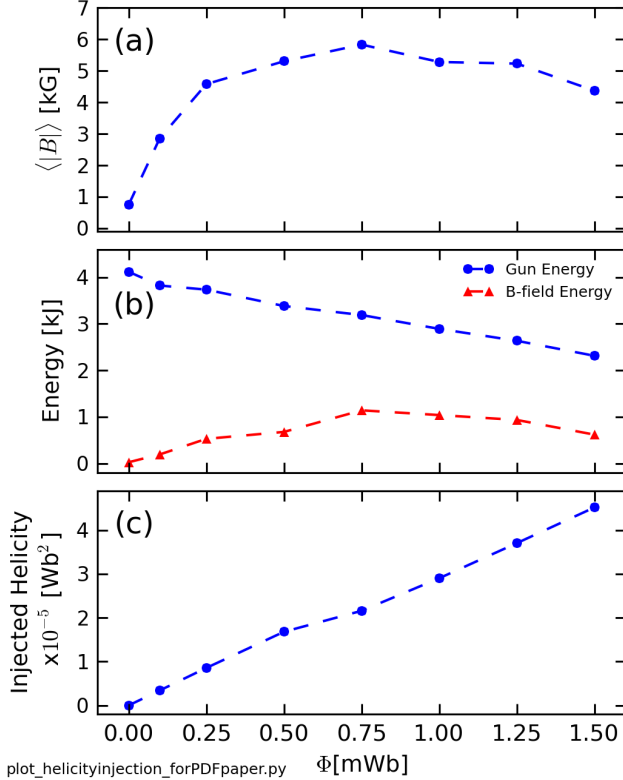


FIG. 2. (a) Average magnetic field magnitude over the equilibrium epoch ( $40\text{--}60\mu s$ ), (b) injected gun energy and volume integrated magnetic field energy, and (c) amount of helicity injected in the first  $20\mu s$  after discharge trigger as a function of magnetic flux in gun core.

The gun voltage is set by a combination of the gun circuit and breakdown physics, but typically does not vary given a particular capacitor charge setting and gas input delay time. Thus, by 2, the injected helicity is modified by the amount of magnetic flux penetrating the gun core. This flux, in turn, is set by the amount of current run through the stuffing coil. The stuffing coil produces magnetic field parallel to the gun axis using a capacitor discharge circuit, but with a much longer timescale than the gun discharge. Because the stuffing coil discharge is much slower, rather than modify the discharge voltage to vary the magnetic field in the gun, the field is set by changing the timing of when the gun fires relative to the

stuffing coil. Thus, changes in flux, and consequently helicity are adjusted by changing the timing delay of the gun trigger.

The amount of flux in the gun core is enhanced by the use of a Permadure<sup>®</sup> in within the gun core. This allows for the flux to be ranged from 0.0 to 1.5 mWb which given a gun voltage of approximately 900V yields an injected helicity range of 0 to  $5 \times 10^{-5} \text{ Wb}^2$  for the first  $20\mu s$ . As indicated in Figure 2(c), the injected helicity scales linearly with the varied magnetic flux. Figure 2(a) and (b) show how the average magnetic field in the center of the chamber and the energy changes with magnetic flux. The magnetic field is determined using a three-axis Bdot probe about 1cm off of the central cylindrical axis, and is time averaged from 40 to  $60\mu s$  which constitutes the equilibrium epoch of the discharge so called as it is the range of most time stationary fluctuations. As Figure 2(a) shows, this value increases initially with flux, but saturates at a value around 5 kG for most flux settings. The gun energy is found by integrating the power,  $P = I_{gun} V_{gun}$ , from 0.0 to  $60.0\mu s$  and represents the maximum amount of energy that can be delivered into the plasma. This value begins around 4 kJ which is about half of the possible circuit energy based on the 1mF, 4.0kV capacitor circuit, and decreases steadily with increasing flux as shown with blue in Fig. 2(b). The amount of energy that actually gets deposited into the magnetic fields is indicated by red in Fig. 2(b), and as would be expected, follows a similar trend as the field magnitude. This energy is calculated by finding the energy density,  $B^2/2\mu_0$ , for each Bdot tip, and integrating over the volume at each radially location.

The power spectrum of magnetic field fluctuations for each helicity case is presented in Figure 3. The curves shown are constructed by taking the a sixth-order Morlet wavelet transform<sup>22</sup> of each  $\dot{B}_r$  timeseries and scaled to  $B_r$  by dividing through by frequency squared. Each curve shows a cascade of power from low frequencies to high frequencies, though the absolute scale in Figure 3(a) has been artificially staggered in order to allow for each curve to be clearly seen. Each spectra exhibits a break-point around 1MHz; a power-law fit is made to the linear region around the break-point for each curve using a Maximum Likelihood Estimation method<sup>23</sup>. The spectral index and error for each fit is indicated in Figure 3. Though the helicity is increasing linearly, the power-law fit for each spectra does not change significantly, hovering around a slope of 3 for low frequency fits and around 5 for high frequency fits. This trend indicates that the change in helicity does not appear to have an effect on the cascade process from larger scales to smaller scales.

The amount of intermittency in the plasma for each helicity state does, however, appear to change. Figure 4 demonstrates how intermittency is determined through the measure of flatness. Fig. 4(a) shows the probability distribution function of increments (PDF) of a time-series at  $2 \times 10^{-5} \text{ Wb}^2$  of injected helicity for two different timescales:  $0.15\mu s$  and  $15\mu s$ . The PDF of increments

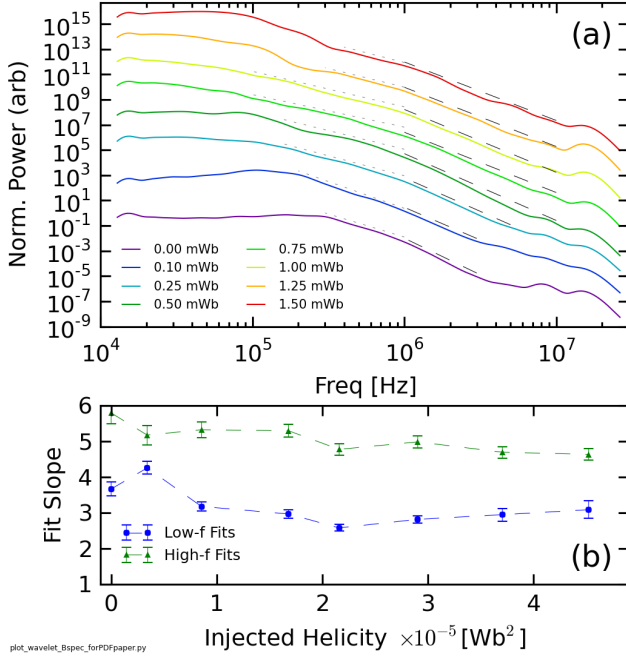


FIG. 3. (a) Wavelet generated magnetic field fluctuation spectra for the radial direction ( $B_r$ ), for each of the eight helicity states. The spectra are staggered in order to highlight the shape of each spectrum. (b) Fits for each spectra for either low or high frequencies. The width in frequency of each fit is indicated by the dashed lines in (a).

is constructed by taking differences of values in a time signal—in this case,  $\dot{B}_r$ —separated by a time scale. As Fig. 4(a) shows, the PDF with small time scale shows a highly pointed PDF with broad, fat tails indicating large excursions from the mean value—or intermittency. This non-Gaussian behavior is indicated by a best-fit Gaussian curve. The PDF with a large time scale increment clearly show a much more Gaussian distribution compared to its best fit. The level of intermittency for each scale can be quantified by taking the normalized fourth-order moment of the PDF—also called flatness or kurtosis. The flatness for each PDF at each timescale, as well as for each helicity state, is shown in Fig. 4(b). Clearly, each state shows increasing flatness, and thus intermittency, with decreasing time scale. The flatness of a purely Gaussian distribution is indicated at  $F=3$ . Moreover, it is observed that the overall flatness of each curve increases as a function of helicity. In other words, the intermittency of the plasma appears to increase with injected helicity.

This change with helicity is summarized in Figure 5(a) where the calculated flatness of each curve in Fig. 4(b) as well as those for  $\dot{B}_\theta$  and  $\dot{B}_z$  has been averaged between the scales indicated by the dashed gray lines: between  $0.1\mu s$  and  $3.0\mu s$ , which approximately corresponds to a frequency range of 333kHz to 10MHz. The average flatness generally increases with helicity, although there is a brief reversal of trend at about  $1 \times 10^{-5} \text{ Wb}^2$  before the curve begins to increase again.

While the physical origin of this observed intermit-

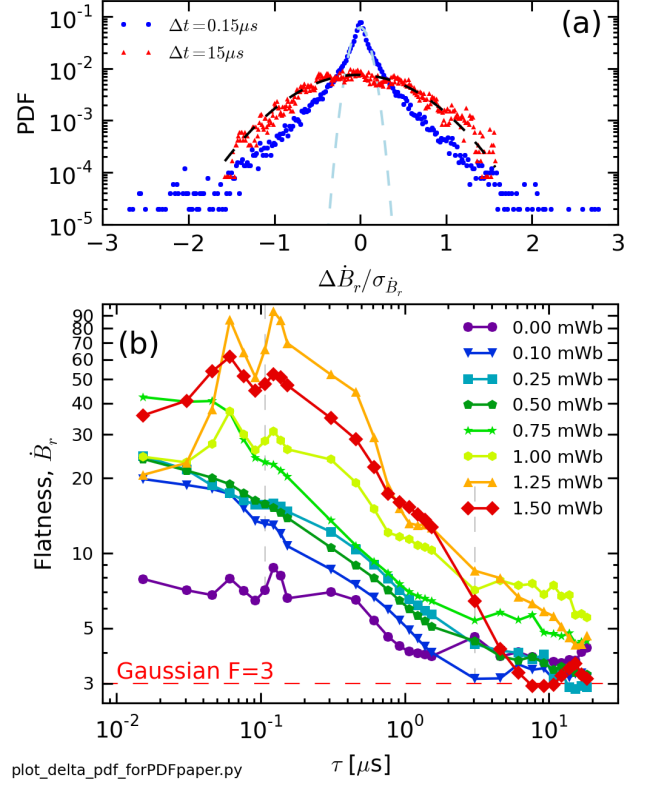


FIG. 4. (a) PDFs for a long and short  $\tau$  from data for  $K_B = 2 \times 10^{-5} \text{ Wb}^2$  indicating the changing in intermittency with timescale. (b) Flatness values for each timescale and each helicity state for the radial  $\dot{B}$  component.

tency and its trend with helicity is not completely understood in the context of this experiment, investigation of intermittency in space plasma yields some possible explanations. Simulations of MHD plasmas modeled after solar wind plasma with time series extracted in ways to match that of *in-situ* satellite observation<sup>8,10,11</sup>, have indicated a correlation between intermittency and the passing of current sheets or reconnection sites. Results on SSX suggest that the appearance and change in observed intermittency can be connected to the changing size and/or frequency of reconnection sites in the plasma. Since many past experiments on SSX have focused on observation of reconnection layers<sup>7</sup>, the machine has a number diagnostics designed to measure signatures of reconnection. These diagnostics are a set soft X-ray photodiodes and the ion doppler spectrometer (IDS) system. The soft X-ray diagnostics is designed to measure X-rays generated by fast tail electrons which were potentially accelerated in the electric field of reconnection sites. Meanwhile, the IDS can measure both burst of ion heating and flow also generated by reconnection events. Fig. 5(b-d) shows the output of these diagnostics for the same helicity scan limited to the same time range as the turbulence data presented above. Soft X-ray measurement shows an initial increase in x-ray light going from zero to small amounts of helicity, but then a consistent decrease in radiation from then on. Fig. 5 shows flatness

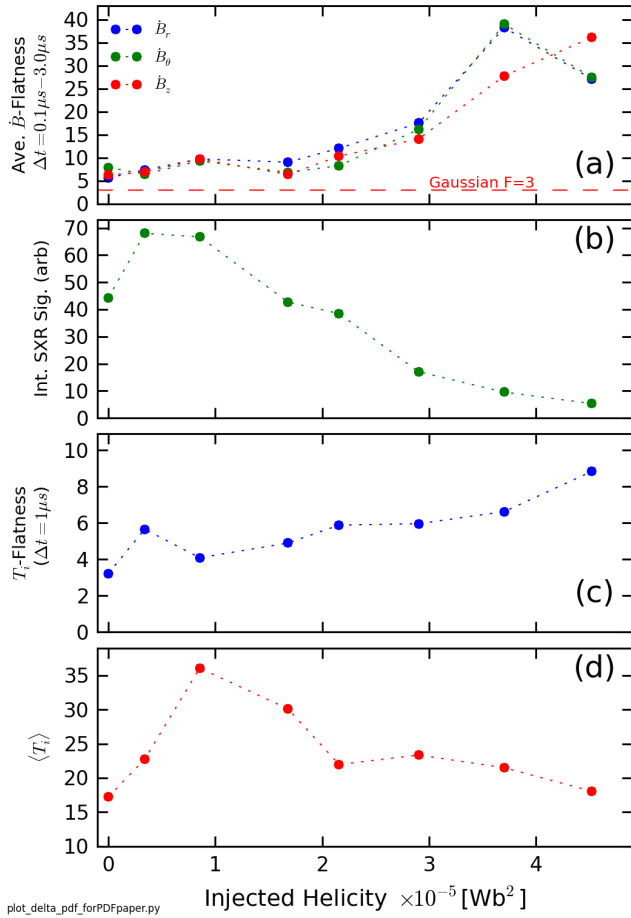


FIG. 5. (a) Average flatness versus helicity. (b) Integrated soft X-ray signal versus helicity. (c) Flatness of  $T_i$  time series versus helicity. (d) Average  $T_i$  versus helicity.

of the ion temperature timeseries as a function of helicity constructed from increment PDFs with a timescale of  $1 \mu\text{s}$ , the minimum timestep available for the IDS system. Like, the flatness curve of  $\hat{B}$ , the ion curve also increases with helicity. Meanwhile, the average measured ion temperature with flatness does not change too much, peaking slightly between  $1$  and  $2 \times 10^{-5} \text{ Wb}^2$ , but generally maintaining a value of between  $20$ - $25 \text{ eV}$ . Though all of these results are somewhat circumstantial, they all fit with the hypothesis of a changing reconnection site size. The decrease in soft X-ray may perhaps be due to decreasing reconnection size as electrons cannot be accelerated to as large as velocities with smaller sites. The increase in ion temperature bursts with little change in the mean ion temperature can arise from a high frequency of reconnection sites. Unlike electrons, the outflow velocity of ions is less likely to be modified by the physical size of the reconnection site.

Unfortunately, since the reconnection diagnostics used here measure line averaged quantities, better evidence for the affect of helicity on reconnection event size cannot be determined as of yet. However, as in solar wind experiments, comparison to simulation may help and studies

using the HiFi simulation are underway.

This paper presents the observation of a clear change in intermittency as a function of injected helicity while simultaneously showing little to no change in the energy transfer rate between scales as indicated by the turbulent power spectra. This discrepancy is perhaps an indication of the need to study higher order moments in turbulence analysis (i.e. 4th order Flatness vs 2nd order spectra) in order to fully flesh out modifications in turbulence. The experiment also demonstrates a straightforward method for modifying the intermittency in a plasma for detailed study. Finally, a possible connection to a physical mechanism was established through soft X-ray and IDS measurements, which suggested the intermittency is related to the spatial size of reconnection sites in the plasma. However, given the limitations of the current diagnostics, any definitive conclusions could not be made, but does provide impetus for further comparison to simulation.

## ACKNOWLEDGEMENTS

We gratefully acknowledge many useful discussions with William Matthaeus. This work has been funded by the US DoE Experimental Plasma Research program and the National Science Foundation. The simulations were performed using the advanced computing resources (Cray XC30 Edison system) at the National Energy Research Scientific Computing Center.

## REFERENCES

- <sup>1</sup>Oieroset, M., *et al.* Direct evidence for a three-dimensional magnetic flux rope flanked by two active magnetic reconnection X-lines at the Earth's magnetopause, *Phys. Rev. Lett.* **107**, 165007, (2011).
- <sup>2</sup>S. Patsourakos, A. Vourlidas, and G. Stenborg. Direct Evidence for a Fast Coronal Mass Ejection Driven by the Prior Formation and Subsequent Destabilization of a Magnetic Flux Rope, *ApJ* **764**, 125, (2013).
- <sup>3</sup>T. Gray, M. R. Brown, and D. Dandurand, Observation of a Relaxed Plasma State in a Quasi-Infinite Cylinder, *Phys. Rev. Lett.* **110**, 085002 (2013).
- <sup>4</sup>J. B. Taylor, *Rev. Mod. Phys.* **58**, 741 (1986).
- <sup>5</sup>W.H. Matthaeus and D. Montgomery, *Ann. N.Y. Acad. Sci.* **357**, 203 (1980).
- <sup>6</sup>Servidio, S., Matthaeus, W. H., and Dmitruk, P.: Depression of Nonlinearity in Decaying Isotropic MHD Turbulence, *Phys. Rev. Lett.* **100**, 095005 (2008).
- <sup>7</sup>Servidio, S., Dmitruk, P., Greco, A., Wan, M., Donato, S., Casak, P. A., Shay, M. A., Carbone, V., Matthaeus, W. H., Magnetic reconnection as an element of turbulence, *Nonlin. Processes Geophys.* **18**, 675-695 (2011).
- <sup>8</sup>Servidio, S., Matthaeus, W. H., Shay, M. A., Cassak, P. A., and Dmitruk, P.: Magnetic Reconnection in Two-Dimensional Magnetohydrodynamic Turbulence, *Phys. Rev. Lett.* **102**, 115003 (2009).
- <sup>9</sup>Servidio, S., Matthaeus, W. H., Shay, M. A., Dmitruk, P., Casak, P. A., and Wan, M.: Statistics of magnetic reconnection in two-dimensional magnetohydrodynamic turbulence, *Phys. Plasmas* **17**, 032315 (2010).

- <sup>10</sup>A. Greco, P. Chuychai, W. H. Matthaeus, S. Servidio and P. Dmitruk, Intermittent MHD structures and classical discontinuities, *Geophys. Res. Lett.* **35**, L19111 (2008).
- <sup>11</sup>Greco, A., Matthaeus, W. H., Servidio, S., Chuychai, P., and Dmitruk, P.: Statistical Analysis of Discontinuities in Solar Wind ACE Data and Comparison with Intermittent MHD Turbulence, *ApJ* **691**, L111 (2009).
- <sup>12</sup>Wan, M., Oughton, S., Servidio, S., and Matthaeus, W. H.: Generation of non-Gaussian statistics and coherent structures in ideal magnetohydrodynamics, *Phys. Plasmas* **16**, 080703 (2009).
- <sup>13</sup>V. S. Lukin and M. G. Linton. Three-dimensional magnetic reconnection through a moving magnetic null. *Nonlin. Processes Geophys.*, 18:871–882, 2011.
- <sup>14</sup>T. R. Jarboe, I. Henins, A. R. Sherwood, Cris W. Barnes, and H. W. Hoida, Slow Formation and Sustainment of Spheromaks by a Coaxial Magnetized Plasma Source, *Phys. Rev. Lett.* **51**, 3942 (1983).
- <sup>15</sup>X. Zhang, D. Dandurand, T. Gray, M. R. Brown, and V. S. Lukin, Calibrated Cylindrical Mach Probe in a Plasma Wind Tunnel, *Rev. Sci. Instr.* **82**, 033510 (2011).
- <sup>16</sup>A. H. Glasser and X. Z. Tang. The SEL macroscopic modeling code. *Comp. Phys. Comm.*, 164:237, 2004.
- <sup>17</sup>V. S. Lukin. *Computational study of the internal kink mode evolution and associated magnetic reconnection phenomena*. PhD thesis, Princeton University, 2008.
- <sup>18</sup>R. Chodura. A hybrid fluid-particle model of ion heating in high-mach-number shock waves. *Nucl. Fusion*, 15:55, 1975.
- <sup>19</sup>A. G. Sgro and C. W. Nieslon. Hybrid model studies of ion dynamics and magnetic field diffusion during pinch implosions. *Phys. Fluids*, 19:126–133, 1976.
- <sup>20</sup>E. T. Meier. *Modeling Plasmas with Strong Anisotropy, Neutral Fluid Effects, and Open Boundaries*. PhD thesis, University of Washington, 2011.
- <sup>21</sup>N. A. Krall and A. W. Trivelpiece. *Principles of Plasma Physics*, chapter Chapter 6: Transport Phenomena in Plasma, pages 311–317. San Francisco Press, Inc., 1986.
- <sup>22</sup>C. Torrence, G.P. Compo, A practical guide to wavelet analysis. *Bull. Am. Meteorol. Soc.* **79**, 6178 (1998).
- <sup>23</sup>A. Clauset, C. Rohilla Shalizi, M.E.J. Newman, Power-law distributions in empirical data, *SIAM Rev.* **51**, 661703 (2009).
- <sup>24</sup>D. Shaikh and P.K. Shukla, 3D Simulations of Fluctuation Spectra in the Hall-MHD Plasma, *Phys. Rev. Lett.* **102**, 045004 (2009).
- <sup>25</sup>Frisch, U. 1995, *Turbulence* (Cambridge: Cambridge Univ. Press)
- <sup>26</sup>M. Wan, K. T. Osman, W. H. Matthaeus, and S. Oughton, Investigation of intermittency in magnetohydrodynamics and solar wind turbulence: scale-dependent kurtosis, *ApJ* **744**, 171 (2012).
- <sup>27</sup>T. Dudok de Wit, O. Alexandrova, I. Furno, L. Sorriso-Valvo, G. Zimbardo, Methods for Characterising Microphysical Processes in Plasmas, *Space Sci. Rev.* **0038-6308**, p. 1-29 (2013).
- <sup>28</sup>Servidio, S., Greco, A., Matthaeus, W. H., Osman, K. T., and Dmitruk, P.: Statistical association of discontinuities and reconnection in magnetohydrodynamic turbulence, *J. Geophys. Res.* **116**, A09102 (2011).
- <sup>29</sup>C. D. Cothran, M. R. Brown, T. Gray, M. J. Schaffer, and G. Marklin, *Phys. Rev. Lett.* **103**, 215002 (2009).
- <sup>30</sup>T. Gray, V. S. Lukin, M. R. Brown, C. D. Cothran, Three-dimensional reconnection and relaxation of merging spheromak plasmas, *Phys. Plasmas* **17**, 102106 (2010).
- <sup>31</sup>T.A. Carter, Intermittent turbulence and turbulent structures in a linear magnetized plasma, *Phys. Plasmas* **13**, 010701 (2006)
- <sup>32</sup>G. Serianni et al 2007 *Plasma Phys. Control. Fusion* **49** B267